

Original Research

## Calcium based siRNA coating: a novel approach for knockdown of *HER2* gene in MCF-7 cells using gold nanoparticles

Abdul Sami<sup>1</sup>, S.M. Saqalan Naqvi<sup>1</sup>, Mazhar Qayyum<sup>2</sup>, Abida Raza Rao<sup>3</sup>, Uteuliyev Yerzhan Sabitaliyevich<sup>4</sup>, M. Sheeraz Ahmad<sup>1\*</sup>

<sup>1</sup> University Institute of Biochemistry and Biotechnology, Pir Mehr Ali Shah, Arid Agriculture University, Rawalpindi, Pakistan

<sup>2</sup> Department of Zoology, Pir Mehr Ali Shah, Arid Agriculture University, Rawalpindi, Pakistan

<sup>3</sup> Nanotheranostic Lab, National Institute of Lasers and Optronics, NILOP, Islamabad, Pakistan

<sup>4</sup> Department of Health Policy and Health Care Development, Kazakh Medical University of Continuing Education, Almaty, Kazakhstan

\*Correspondence to: [dr.sheeraz@uaar.edu.pk](mailto:dr.sheeraz@uaar.edu.pk)

Received January 10, 2020; Accepted June 16, 2020; Published September 30, 2020

Doi: <http://dx.doi.org/10.14715/cmb/2020.66.6.19>

Copyright: © 2020 by the C.M.B. Association. All rights reserved.

**Abstract:** Surface functionalization of nanoparticles (NPs) for therapeutic siRNA delivery into cancer cells has gained interest. The present study was designed for surface functionalization of gold nanoparticles (AuNPs) for efficient siRNA delivery and knockdown in cancer cells. In order to achieve this objective, AuNPs were coated with *HER2*-siRNA in the presence of 11-mercaptoundecanoic acid (11-MUA), calcium chloride (CaCl<sub>2</sub>) and polyethyleneimine (PEI) in alternate charge bearing successive layers. MCF-7 cells were cultured and transfected with fabricated assembly of AuNPs. Cytotoxicity analysis revealed that the half inhibitory concentration (IC<sub>50</sub>) for the formulation was 45.35 nM. Total RNA was isolated from transfected cells, reverse transcribed into complementary DNA (cDNA) and real-time polymerase chain reaction (RT-PCR) was performed. The RT-PCR based delta-delta Ct analysis in treated cells revealed a significant 18.94 times decrease ( $p < 0.001$ ) in the expression of *HER2* gene standardized with *ACTB* housekeeping gene as compared to untreated cells, which makes this formulation a potent approach for siRNA delivery and gene knockout.

**Key words:** Gold nanoparticles; *HER2*; siRNA silencing; MCF-7.

### Introduction

Cancer is one of the major causes of death worldwide. Globally, every 1 in 6 deaths is related to cancer and the number is still expected to increase (1). In cancer, cells of the body start dividing uncontrollably and this abnormal division is triggered by mutation in either proto-oncogenes or tumor suppressor genes, resulting in the loss of cell cycle regulation and increased proliferation (2). Traditional strategies for cancer treatment include surgery in conjunction with chemo and/or radiotherapy. Success ratio of these traditional therapeutic methods is not very high and requires cancer to be diagnosed earlier. Gene therapy provides an excellent way to target cancer, especially via gene silencing of up-regulated oncogenes (3). RNA interference (RNAi) is being used to modulate gene expression by utilizing the small fragments of double stranded RNA (dsRNA) molecules including short hairpin RNA (shRNA), endogenous microRNA (miRNA), and small interfering RNA (siRNA). The most utilized one is siRNA due to the ease of synthesis and no requirement of genome integration (4,5). Accomplishment of siRNA mediated specific gene silencing requires its effective delivery into target cells. (6–8). There are possibly thousands of materials that can be complexed with siRNA for its delivery into cells. For example, lipid based liposomal nanoparticles, PEI based complexes, calcium based complexes and AuNPs

and other metallic NP based complexes (9–11). Out of these, choice must be made to select a material with effective complexing abilities with nucleic acids and must be biocompatible and less cytotoxic. AuNPs serve as a striking tool for nucleic acid delivery (12). Advantages of using AuNPs include their synthesis in required size with narrow size distribution range, mono dispersity, surface modification for creation of multifunctional monolayers to allow multiple moieties such as nucleic acids and targeting agents to be attached (13). Furthermore, they impart little cytotoxicity and efficient bio-distribution in targeted cells (14,15). However, AuNPs require certain biocompatible polymer conjugated to the surface in order to facilitate their endocytosis. PEI is one of the commonly utilized polymer for nucleic acid delivery into cell via endocytosis, but it is cytotoxic to cells and cytotoxicity depends upon many factors including its concentration, degree of branching and unbranching, molecular weight and zeta potential (16,17). On the other hand, calcium related salts have been extensively studied as non-viral vectors for gene delivery, due to their inherent use as a compositional part of bones and teeth (18). They have excellent biocompatibility and play roles in cellular uptake mechanisms via endocytosis (19). They have high affinity to bind a variety of biomolecules making it suitable for formation of complexes with biomolecules like insulin, growth factors and nucleic acids (20–22). In the present study, we uti-

lize AuNPs to fabricate a complex of calcium and PEI in layer by layer assembly to deliver siRNA against *HER2* into breast cancer MCF-7 cell line. We demonstrate the successful delivery of siRNA through AuNPs and calcium-based formulation assembly for knocking down the expression of *HER2* gene.

## Materials and Methods

### Synthesis and characterization of AuNPs

Gold nanoparticles were synthesized by citrate reduction method (23). 20 mL of 1.0 mM hydrogen tetrachloroaurate ( $\text{HAuCl}_4$ ) was boiled, 2 mL of 1% solution of trisodium citrate dihydrate ( $\text{Na}_3\text{C}_6\text{H}_5\text{O}_7 \cdot 2\text{H}_2\text{O}$ ) was added to boiling solution of  $\text{HAuCl}_4$ . After 10 minutes of boiling, citrate reduced gold ions and AuNPs were produced turning suspension in deep cherry red color. Particles were characterized by scanning electron microscopy (SEM) (Joel instruments) and dynamic light scattering (DLS) method via Nanosizer (Malvern instruments) for size, hydrodynamic diameter and surface charge.

### siRNA and primer sequences

Sequence of *HER2*-siRNA and PCR primers used in this study are shown in table 1.

### Layer by layer assembly of *HER2*-siRNA/AuNPs formulation

*HER2* sense and antisense siRNA were re-suspended and annealed in annealing buffer. 0.1 mg/mL solution of 11-MUA, 0.5 mg/mL solution of PEI (25kDA, Branched), 2 M solution of  $\text{CaCl}_2$  were made separately and filtered sterilized using 0.2  $\mu\text{m}$  syringe filters. For the first layer of coating, 0.2 mg/mL NPs were obtained in 1.5 mL centrifuge tube in total volume of 500  $\mu\text{L}$ . 11-MUA was added at 0.1 mg/mL, incubated for 30 minutes at room temperature and centrifuged at 16000 x g twice for 5 minutes to remove unbound 11-MUA and mixed in 100  $\mu\text{L}$ , 10 mM NaCl solution. For the second layer, 2 M  $\text{CaCl}_2$  was added to AuNPs from previous step and incubated for 30 minutes followed by centrifugation at 16000 x g twice for 5 minutes to remove unbound  $\text{CaCl}_2$  and mixed in 100  $\mu\text{L}$ , 10 mM NaCl solution. For the third layer, 2.1  $\mu\text{M}$  *HER2*-siRNA was added to AuNPs from previous step and incubated for 30 minutes followed by centrifugation at 16000 x g twice for 5 minutes to remove unbound siRNA and mixed in 100  $\mu\text{L}$ , 10 mM NaCl solution. For fourth and final layer of *HER2*-siRNA/AuNPs formulation, 1.0 mg/mL PEI was added to AuNPs from previous step and incubated for 30 minutes followed by centrifugation at 16000 x g twice for 5 minutes to remove unbound PEI and mixed

in 100  $\mu\text{L}$ , 10 mM NaCl solution (Fig. 1). After addition of each layer, the formulation was subjected to spectral scan via UV-VIS spectrophotometry to determine the peak plasmon shift.  $\zeta$  potential was also determined after addition of each layer to confirm the charge reversal by each polymer.

### siRNA release profile

After the preparation of NPs formulation, the release profile of siRNA was characterized. In order to determine the release profile, 1 mL of formulation was incubated in 3mL of phosphate buffer saline (PBS, pH 7.3-7.4) at 37 °C at different time intervals for up to 144 hours. The samples were centrifuged at 13,000 x g for 30 min at 37°C and resulting pellets were re-suspended in 3mL of PBS after each designated time interval. The supernatant from each centrifugation step was used to check for the presence of released siRNA by measuring absorbance at 260nm via UV spectrophotometry. The amount in the supernatant was then subtracted from the initial amount loaded to determine the amount released at a given time point.

### Cytotoxicity assay

MCF-7 cells were grown in Dulbecco's Modified Eagle Media (DMEM), with 10 % fetal bovine serum (FBS) and 1% penicillin/streptomycin, 0.1 mM L-glutamine, 1.0 mM sodium pyruvate with 2.4 g/L sodium bicarbonate in T25 cell culture flasks in a humidified  $\text{CO}_2$  incubator at 37°C. After sub culturing the cells were plated in 24 well plate at cell count of  $2.5 \times 10^4$  cells per well for transfection studies and incubated in humidified  $\text{CO}_2$  incubator at 37°C. 100  $\mu\text{L}$  of complex was mixed with serum free 150  $\mu\text{L}$  medium. Mix was incubated for 5 minutes before adding to the cells after removing the older complete growth medium. After addition of complex in triplicates, plates were incubated in humidified incubator at 37°C for 48 hours. MTT cytotoxic assay was performed according to instruction provided by manufacturer.

### RNA isolation and cDNA synthesis

MCF-7 cells were separately transfected with AuNPs formulation. After 48 hours of transfection, cells were trypsinized, washed with phosphate buffer saline (PBS)

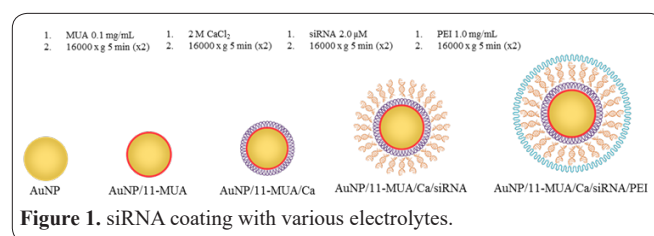


Figure 1. siRNA coating with various electrolytes.

Table 1. Sequence of siRNA and primers of *HER2* and *ACTB*.

Gene Name	Sequence
<i>HER2</i> -siRNA Sense strand	5'-rCrArArArUrGrUrUrGrGrArUrGrArUrUrGrArCrUrCrUrGAA-3'
<i>HER2</i> -siRNA Anti-sense strand	5' rUrUrCrArGrArGrUrCrArArUrCrArUrCrCrArArCrArUrUrUrGrArC -3'
<i>HER2</i> -forward primer	5'-GGGAAACCTGGAACCTCACCT-3'
<i>HER2</i> -reverse primer	5'-CCCTGCACCTCCTGGATA-3'
<i>ACTB</i> -forward primer	5'- GGATCAGCAAGCAGGAGTATG -3'
<i>ACTB</i> -reverse primer	5'- AGAAAGGGTGTAACGCAACTAA -3'

and collected in micro centrifuge tubes. Total RNA was isolated using TRIzol® Plus RNA Purification Kit from Thermo Fisher according to protocol. Purified RNA was stored at - 80°C. cDNA was synthesized by Maxima First Strand cDNA Synthesis Kit (Thermo Fisher) according to the manufacturer protocol.

### Gene expression profiling by quantitative real-time PCR

To determine the level of mRNA in transfected and untreated cells, cDNA was subjected to qPCR using 5x HOT FIREPol® EvaGreen® qPCR Mix Plus according to the manufacturer protocol with following thermal profile: initial activation for 12 min at 95°C, denaturation for 30 seconds at 95°C, annealing for 30 seconds at 52°C for *HER2* and 57°C for *ACTB* respectively, elongation for 30 seconds at 72°C, thermal profile was run 40 times from denaturation to elongation. The green/FAM channel was selected for EvaGreen fluorescence detection. The Ct values data were subjected to  $2^{-\Delta\Delta Ct}$  analysis to find out fold change.

## Results

### Characterization of nanoparticles

The average hydrodynamic diameter of spherical AuNPs measured by DLS was 34.44 nm and the polydispersity index (PDI) was  $0.117 \pm 0.002$  as shown in histogram (Fig. 2).

The surface charge or zeta ( $\zeta$ ) potential was  $-12 \pm 1.75$  mVolts. AuNPs were subjected to UV-VIS spectrophotometry to obtain spectral scan which showed maximum absorption peak at  $521 \pm 2$  nm (Fig. 3), thus confirming the presence of gold in suspension. Finally, SEM images confirmed the presence of AuNPs with an average diameter of  $21.8 \pm 1.3$  nm (Fig. 4). It is worth noting that NPs size varied when measured with nanosizer, this is because of the difference in the working principles of these instruments. Nanosizer measures the hydrodynamic diameter by light intensity scattered by an object/nanoparticle in light path and average size is calculated based upon solution dynamics of particles. On the other hand, SEM yields images of individual particles and it is considered more suitable for metallic nanoparticles (24).

### Layer by Layer assembly of *HER2*-siRNA/AuNP complex

AuNPs were coated with 11-MUA, Ca, siRNA and PEI successively. Addition of each charge bearing successive layer resulted in the shift of plasmon peak from 520 nm to 535 nm (Fig. 5) which indicated the addition of respected layer. Furthermore, the intensity of absorbance of bare AuNPs was reduced from 0.087 to 0.05 which showed that the AuNPs are being covered evenly by layers of charged polymers (Fig. 6). The surface charge analysis of each successive layer revealed that bare AuNPs had slight negative charge of -1 to -5 mV due to presence of negatively charged citrate ions. The addition of 11-MUA resulted in the even distribution of negative charge in the surface of AuNPs with -17 mV. Ca rendered the formulation with +19 mV charge while addition of negatively charged *HER2*-siRNA contributed to -20 mV and final layer of PEI provided +23 mV

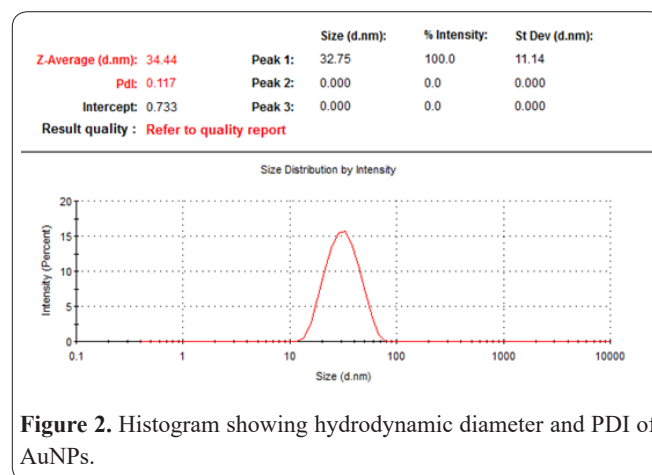


**Figure 2.** Histogram showing hydrodynamic diameter and PDI of AuNPs.

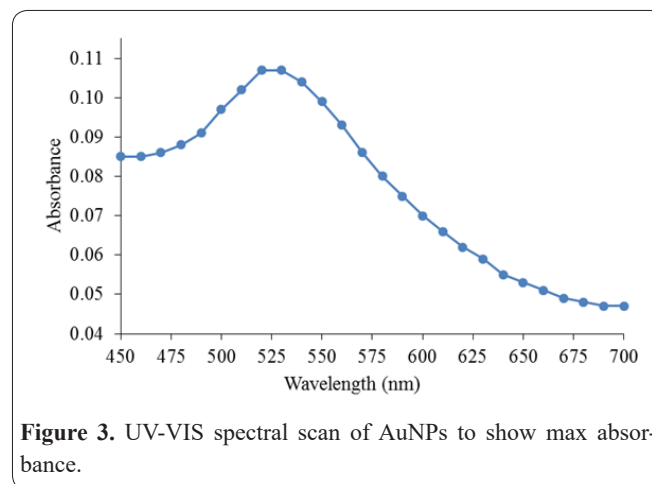


**Figure 3.** UV-VIS spectral scan of AuNPs to show max absorbance.

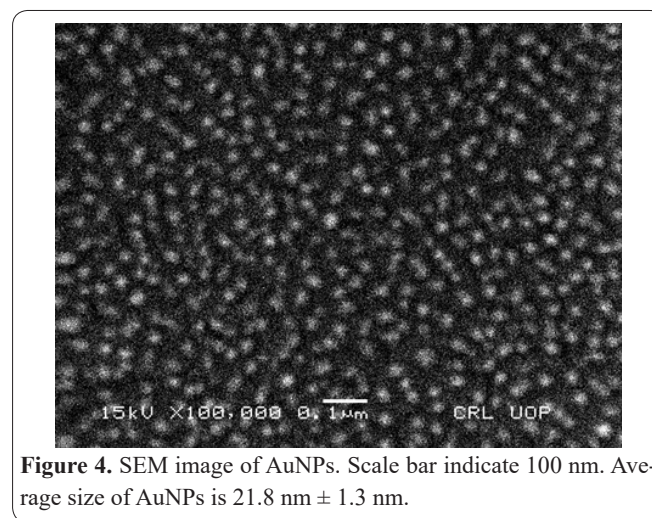


**Figure 4.** SEM image of AuNPs. Scale bar indicate 100 nm. Average size of AuNPs is  $21.8 \text{ nm} \pm 1.3$  nm.

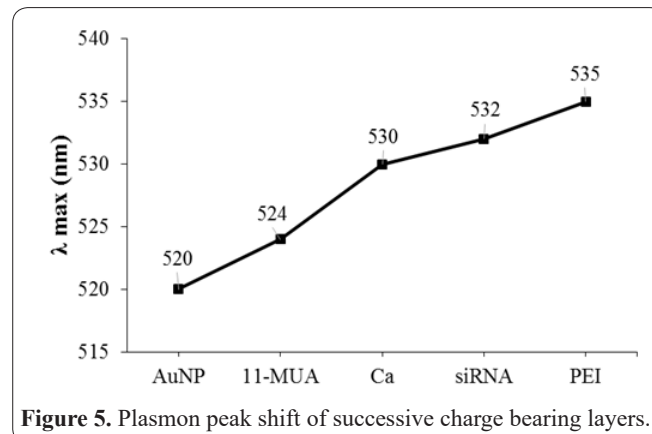


**Figure 5.** Plasmon peak shift of successive charge bearing layers.

surface charge which would facilitate the entry of formulation in MCF-7 cells (Fig. 7).

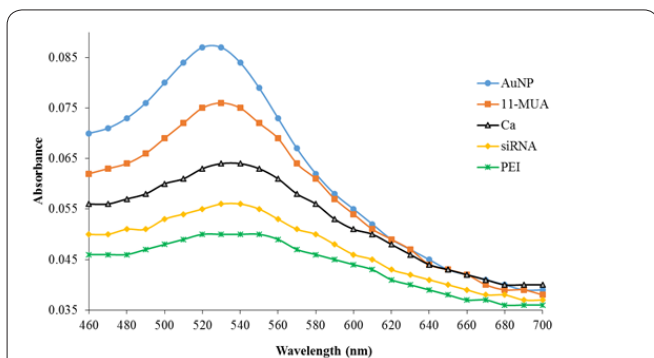


**Figure 6.** UV-VIS spectral scan of successive charge bearing layers.

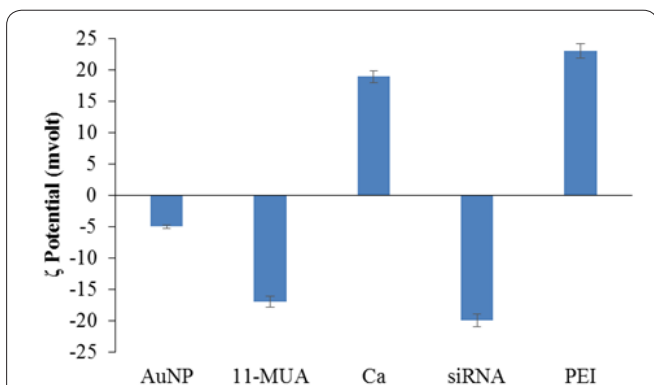


**Figure 7.** Charge reversal of various polymers.

### siRNA release profile

Release profile of formulation was assessed by measuring the absorbance of released siRNA in supernatant at 260nm via UV-Vis spectrophotometry. siRNA release was assessed at different time intervals of 6, 12, 24, 48, 96, 120 and 144 hours. The results indicated that after 6 hours of incubation 60% siRNA was released from the formulation. After 12 hours of incubation 76% and after 24 hours 82% siRNA was released. This showed that the significant amount (more than 80%) of siRNA was released in early few hours. In the later hours the siRNA release was at much slower rate and 95% of siRNA was released up till 144 hours (Fig. 8). This quick liberation of siRNA might be attributed to the fact that Ca is a divalent ion and the electrostatic interactions between Ca ions and siRNA are relatively weaker (25,26).

### Assessment of cellular uptake of formulation into cancer cells with *EGFP* plasmid

In order to assess the cellular uptake of formulation in MCF-7 cells, *EGFP* plasmid (Addgene plasmid #13031) was coated on AuNPs instead of *HER2*-siRNA just to confirm the entry of fabricated particles into the cells. *EGFP* plasmid was conjugated with lipofectamine2000 to serve as positive control for cellular uptake in MCF-7 cells and *EGFP* plasmid with no carrier was used to serve as negative control. After 48 hours of transfection with AuNP-*EGFP*, positive and negative control, MCF-7 cells were fixed using 4% paraformaldehyde and imaged with fluorescence microscope for the presence of fluorescence produced by green fluorescence protein (GFP) expressed by *EGFP* plasmid. Our results indicated the presence of fluorescence of GFP in both positive control (Fig. 9) and AuNP-*EGFP* formulation (Fig. 10). These results indicated that our formulation is capable

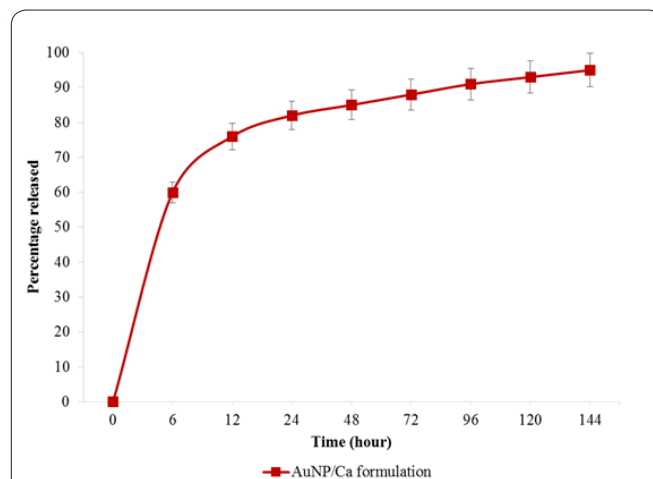


**Figure 8.** Release of siRNA molecules from the formulation in PBS at different time intervals. Error bars represent 5% standard error (n=3).

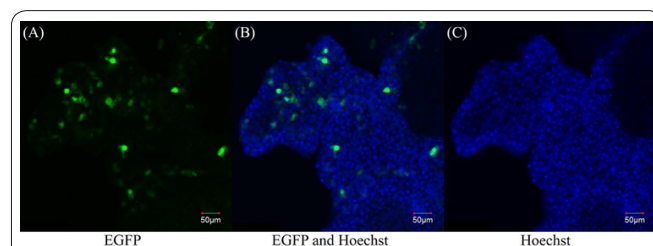


**Figure 9.** Fluorescent microscope image of MCF-7 cells transfected with *HER2*-siRNA/lipofectamine2000 as positive control. Image (A) showing fluorescence of EGFP while image (B) showing EGFP merged on to Hoechst and image (C) showing Hoechst only.

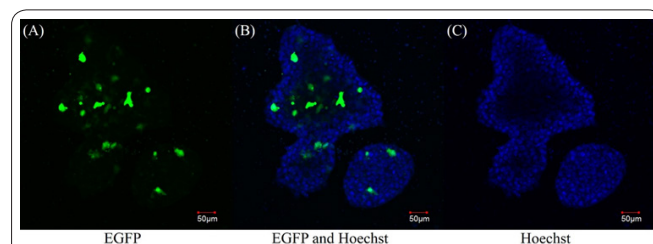
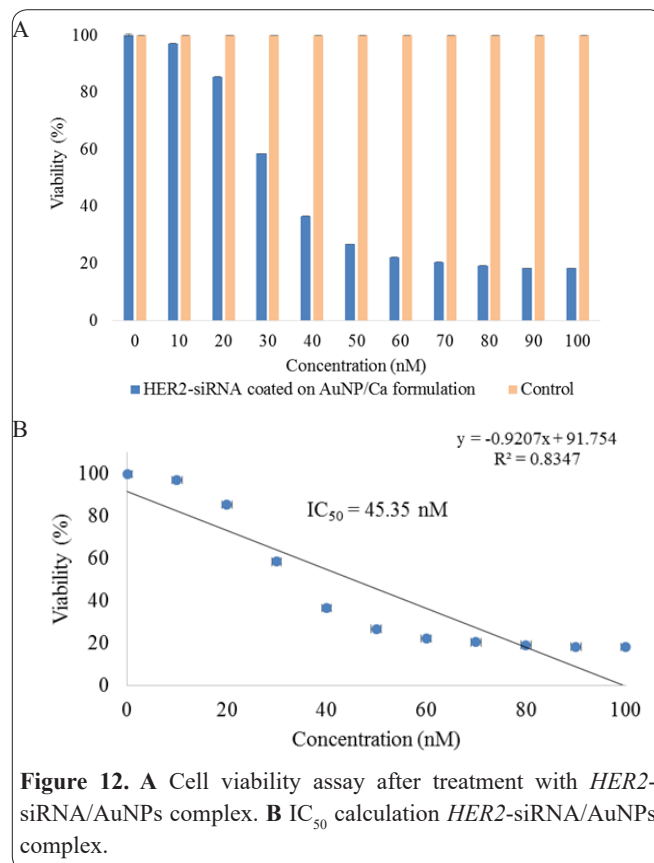
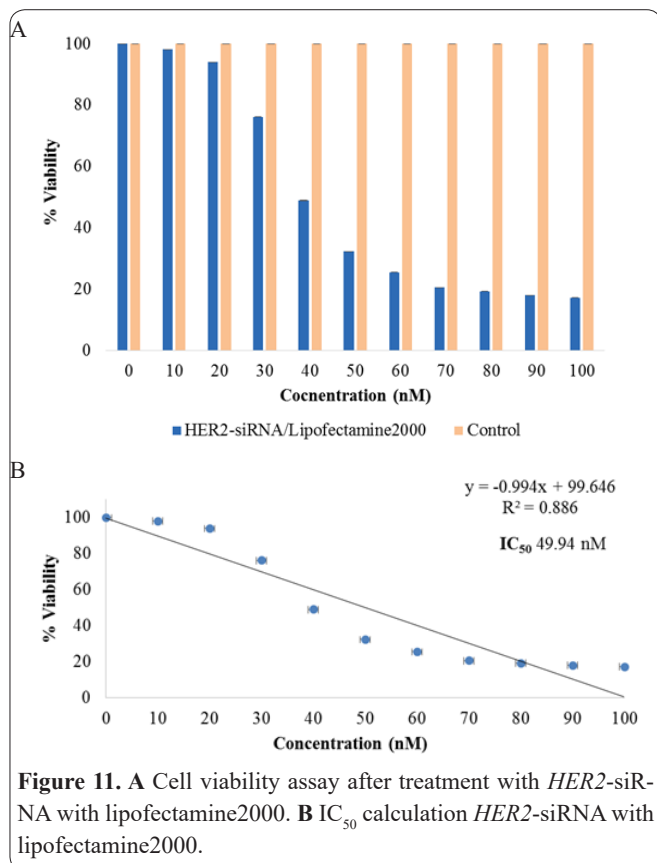


**Figure 10.** Fluorescent microscope image of MCF-7 cells transfected with *HER2*-siRNA/AuNPs formulation. Image (A) showing fluorescence of EGFP while image (B) showing EGFP merged on to Hoechst and image (C) showing Hoechst only.

of carrying nucleic acids into the cells.

### Cytotoxicity assessment of formulation

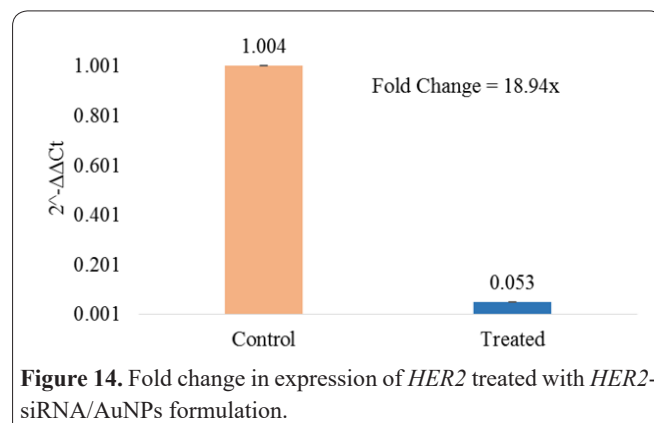
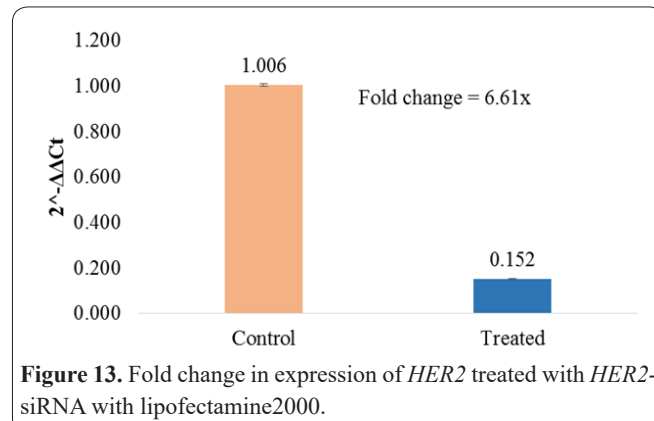
MCF-7 cells were transfected with variable concentrations of NPs formulation and lipofectamine2000 conjugated with *HER2*-siRNA serving as positive control to assess the cytotoxicity. *HER2*-siRNA alone with no carrier served as negative control. The results showed decrease in the viability of cells at various concentrations. In lipofectamine2000 formulation cell viability decreased from 100% to 20% with concentration of 10 nM to 70 nM. Increase in the concentration of beyond 70 nM did not show any notable change. The half maximum inhibitory value ( $IC_{50}$ ) was calculated to be  $49.94 \text{ nM} \pm 0.1$  (n=3). (Fig. 11a, 11b). The cells treated with siRNA conjugated with AuNPs in Ca formulation showed the dose dependent decrease in the cell viability. Viability assessment of AuNPs with *HER2*-siRNA treated cells showed that at 10nM concentra-



tion, 97.11% cells were viable which were decreased to 85% at the concentration of 20nM. An obvious change in decreased viability was found at 30nM concentration when 58% cells were found viable. Viability of cells was further decreased to 36.5% at concentration of 40nM. When concentration was increased to 50nm, viability was further decreased to 26.7% and it became 22.2% at the concentration of 60nM. Little bit decrease in viability was observed at the concentration of 70nM i.e. 20%. It could be seen from results that an obvious decrease has been found between concentrations of 20nm to 40nM when viability was decreased from 85% to 36.5%. Beyond 60nM observed change was negligible (Figure 12a, 12b). The  $IC_{50}$  was  $45.35\text{ nM} \pm 0.1$  ( $n=3$ ). These results indicated that the *HER2*-siRNA/AuNPs formulation has slightly higher cytotoxicity at relatively lower concentration as compared to positive control.

### Gene expression analysis

The expression analysis on MCF-7 cell treated with 100 nM (2X of  $IC_{50}$ ) of *HER2*-siRNA/lipofectamine2000 (positive control) and 91 nM (2X of  $IC_{50}$ ) of *HER2*-siRNA/AuNPs was performed. Results of cells treated with positive control showed that  $2^{-\Delta\Delta Ct}$  values for the treated and untreated cells were 0.152 and 1.006 respectively. This revealed a significant decrease ( $p<0.001$ ) in the expression of *HER2* gene when compared to untreated cells and fold decrease in the expression of *HER2* was 6.61 times. (Fig. 13). On the other hand, MCF-7 cell treated with *HER2*-siRNA/AuNPs showed  $2^{-\Delta\Delta Ct}$  values of 1.004 and 0.053 in treated and untreated cells respectively. This also led to the significant decrease ( $p<0.001$ ) in the expression of *HER2* by 18.94 times (Fig. 14).



### Discussion

RNAi mediated gene silencing has appeared as a powerful strategy in handling cancer producing genes by complementary base-pairing mechanism (27). siRNA is a very important tool with substantial use in cancer therapy (28). Specifically, designed siRNA has the ability to modify the expression of cancer-causing

genes by homology-based pairing and post-transcriptional silencing. siRNA is a powerful tool to knockdown the oncogenes due to its specific and efficient silencing of target mRNAs (29). As previously reported, the efficiency and specificity of siRNA could be enhanced with the help of NPs as carriers (30), which have emerged as a striking tool for the delivery of biomolecules due to their easy synthesis, good biocompatibility, ready functionalization and monodispersity (31,32). This could be clearly observed in our results. The formulation successfully killed MCF-7 cells with an  $IC_{50}$  of 45.35 nM while the  $IC_{50}$  of siRNA conjugated with lipofectamine2000 was 49.94 nM. This indicates a higher degree of cell death when siRNA was conjugated in layer by layer assembly, probably due to the slow and steady release and greater half-life of siRNAs that resulted in suppression of MCF-7 cells proliferation. Furthermore, in terms of gene expression analysis, our results showed that with lipofectamine2000, the expression of *HER2* was reduced by 6.1 times, while *HER2*-siRNA/AuNPs complex reduced the expression of *HER2* by 18.94 times, indicating a greater efficiency of AuNPs in siRNA delivery to the cells. These results are consistent with previous finding which showed that AuNPs, due to inert character of metallic gold are non-toxic, form fine NPs with easy functionalization provide safer and efficient means of siRNA delivery (33). These results also confirm the efficiency of siRNA in knockdown of oncogene with AuNPs delivery system, indicating the therapeutic role of siRNA and NPs in cancer models (34,35). Furthermore, the previous studies showed that after introduction of the layer by layer technology for siRNA-AuNPs delivery into the cell by Elbakry *et al.* (2009). PEI was used as a gold standard for gene delivery but PEI is cytotoxic itself. (36,37). Due to additional cytotoxicity conferred by PEI, we used calcium in our formulation as AuNPs/MUA/Ca/siRNA/PEI. The application of calcium-based biomaterials in gene delivery causes calcium ion to form ionic complexes with the helical phosphates of DNA, and these complexes have easy transportability across the cell membrane via ion channel-mediated endocytosis. (38). Our results indicated that this formulation worked efficiently.

In conclusion, The present study shows calcium-based layer by layer assembly of siRNA-AuNPs silencing complex which successfully delivered *HER2*-siRNA into MCF-7 cells and efficient knockdown of *HER2* gene. The RT-PCR based delta-delta Ct analysis in treated cells revealed a significant 18.94 times decrease ( $p < 0.001$ ) in the expression of *HER2* gene standardized with *ACTB* housekeeping gene as compared to untreated cells, which makes this formulation a promising approach. Based on the results it is suggested that in future, the formulation should be tested in the xenografted mice models to evaluate its delivery and knockout potential in-vivo.

#### Acknowledgement

The funding for this research was provided by Higher Education Commission (HEC), Pakistan under Indigenous PhD Fellowship.

#### Conflict of Interest

The Authors declare no conflict of interest for this publication.

cation.

#### References

1. World Health Organization. WHO | Cancer Factsheet. WHO 2018.
2. Deng Y, Wang CC, Choy KW, Du Q, Chen J, Wang Q, et al. Therapeutic potentials of gene silencing by RNA interference: Principles, challenges, and new strategies. *Gene* 2014; 53: 217–27.
3. Duarte S, Carle G, Faneca H, Lima MCP de, Pierrefite-Carle V. Suicide gene therapy in cancer: Where do we stand now? *Cancer Lett* 2012; 324(2):160–70.
4. Guo W, Chen W, Yu W, Huang W, Deng W. Small interfering RNA-based molecular therapy of cancers. *Chinese Journal of Cancer* 2013; 32: 488–93.
5. Xu C, Wang J. Delivery systems for siRNA drug development in cancer therapy. *Asian J Pharm Sci* 2015; 10(1):1–12.
6. Aagaard L, Rossi JJ. RNAi therapeutics: Principles, prospects and challenges. 59, *Advanced Drug Delivery Reviews* 2007; 59:75–86.
7. Whitehead KA, Langer R, Anderson DG. Knocking down barriers: Advances in siRNA delivery. *Nature Reviews Drug Discovery* 2009; 8:129–38.
8. Juliano R, Alam MR, Dixit V, Kang H. Mechanisms and strategies for effective delivery of antisense and siRNA oligonucleotides. *Nucleic Acids Res* 2008; 36(12):4158–71.
9. Zhang S, Zhao B, Jiang H, Wang B, Ma B. Cationic lipids and polymers mediated vectors for delivery of siRNA. *Journal of Controlled Release* 2007; 123:1–10.
10. Khosravi DK, Mozafari MR, Rashidi L, Mohammadi M. Calcium based non-viral gene delivery: An overview of methodology and applications. *Acta Medica Iranica* 2010; 48: 133–41.
11. Li X, Xu H, Li C, Qiao G, Farooqi AA, Gedanken A, et al. Zinc-doped copper oxide nanocomposites inhibit the growth of pancreatic cancer by inducing autophagy through AMPK/mTOR pathway. *Front Pharmacol* 2019; 10: 319-325.
12. Boisselier E, Astruc D. Gold nanoparticles in nanomedicine: Preparations, imaging, diagnostics, therapies and toxicity. *Chemical Society Reviews* 2009; 38(6):1759-82.
13. Bowman MC, Ballard TE, Ackerson CJ, Feldheim DL, Margolis DM, Melander C. Inhibition of HIV fusion with multivalent gold nanoparticles. *J Am Chem Soc* 2008; 130 (22):6896–7.
14. Zhu ZJ, Carboni R, Quercio MJ, Yan B, Miranda OR, Anderton DL, et al. Surface properties dictate uptake, distribution, excretion, and toxicity of nanoparticles in fish. *Small* 2010; 18(20):2261-5.
15. De Jong WH, Hagens WI, Krystek P, Burger MC, Sips AJAM, Geertsma RE. Particle size-dependent organ distribution of gold nanoparticles after intravenous administration. *Biomaterials* 2008; 29(12):1912-9.
16. Lungwitz U, Breunig M, Blunk T, Göpferich A. Polyethylenimine-based non-viral gene delivery systems. *Euro Jou of Pharma and Biopharma* 2005; 60(2):247–66.
17. Kim YH, Park JH, Lee M, Kim YH, Park TG, Kim SW. Polyethylenimine with acid-labile linkages as a biodegradable gene carrier. *J Control Release* 2005; 103(1):209–19.
18. Zhang S, Gonsalves KE. Preparation and characterization of thermally stable nanohydroxyapatite. *J Mater Sci Mater Med* 1997; 8(1):25–8.
19. Schmidt HT, Gray BL, Wingert PA, Ostafin AE. Assembly of aqueous-cored calcium phosphate nanoparticles for drug delivery. *Chem Mater* 2004; 16(24):4942–7.
20. Chen C, Okayama H. High-efficiency transformation of mammalian cells by plasmid DNA. *Mol Cell Biol* 1987; 7(8):2745–52.

21. Ralec C, Henry E, Lemor M, Killelea T, Henneke G. Calcium-driven DNA synthesis by a high-fidelity DNA Polymerase. *Nucleic Acids Res* 2017; 45(21):12425–40.
22. Antipina AY, Gurtovenko AA. Molecular mechanism of calcium-induced adsorption of DNA on zwitterionic phospholipid membranes. *J Phys Chem B* 2015; 119(22):6638–45.
23. McFarland AD, Haynes CL, Mirkin C a., Van Duyne RP, Godwin H a. Color My Nanoworld. *J Chem Educ* 2004; 81(4):544A. <http://dx.doi.org/10.1021/ed081p544A%5Cnhttp://pubs.acs.org/doi/abs/10.1021/ed081p544A%5Cnhttp://pubs.acs.org/doi/pdf/10.1021/ed081p544A>
24. Eaton P, Quaresma P, Soares C, Neves C, de Almeida MP, Pereira E, et al. A direct comparison of experimental methods to measure dimensions of synthetic nanoparticles. *Ultramicroscopy* 2017; 182:179–90.
25. Ziebarth JD, Kennetz DR, Walker NJ, Wang Y. Structural Comparisons of PEI/DNA and PEI/siRNA Complexes Revealed with Molecular Dynamics Simulations. *J Phys Chem B* 2017; 121(8):1941–52.
26. Ruvinov E, Kryukov O, Forti E, Korin E, Goldstein M, Cohen S. Calcium-siRNA nanocomplexes: What reversibility is all about. *J Control Release* 2015; 203:150–60.
27. Mansoori B, Shotorbani SS, Baradaran B. RNA interference and its role in cancer therapy. *Advanced Pharmaceutical Bulletin* 2014; 4:313–21.
28. Senapati D, Patra BC, Kar A, Chini DS, Ghosh S, Patra S, et al. Promising approaches of small interfering RNAs (siRNAs) mediated cancer gene therapy. *Gene* 2019; 719:1-12.
29. Santarius T, Shipley J, Brewer D, Stratton MR, Cooper CS. A census of amplified and overexpressed human cancer genes. *Nature Reviews Cancer* 2010; 10:59–64.
30. Williford J-M, Wu J, Ren Y, Archang MM, Leong KW, Mao H-Q. Recent Advances in Nanoparticle-Mediated siRNA Delivery. *Annu Rev Biomed Eng* 2014; 16:347-70.
31. Lee JS, Green JJ, Love KT, Sunshine J, Langer R, Anderson DG. Gold, poly( $\beta$ -amino ester) nanoparticles for small interfering RNA delivery. *Nano Lett* 2009; 6:2402–06.
32. Nogueira DR, Scheeren LE, Macedo LB, Marcolino AIP, Pilar Vinardell M, Mitjans M, et al. Inclusion of a pH-responsive amino acid-based amphiphile in methotrexate-loaded chitosan nanoparticles as a delivery strategy in cancer therapy. *Amino Acids* 2016; 1:157-68.
33. Giljohann DA, Seferos DS, Prigodich AE, Patel PC, Mirkin CA. Gene regulation with polyvalent siRNA-nanoparticle conjugates. *J Am Chem Soc* 2009; 131(6):2072–73.
34. Cui D, Zhang C, Liu B, Shu Y, Du T, Shu D, et al. Regression of Gastric Cancer by Systemic Injection of RNA Nanoparticles Carrying both Ligand and siRNA. *Sci Rep* 2015; 15:1-14.
35. McCarroll JA, Dwarte T, Baigude H, Dang J, Yang L, Erlich RB, et al. Therapeutic targeting of polo-like kinase 1 using RNA-interfering nanoparticles (iNOPs) for the treatment of non-small cell lung cancer. *Oncotarget* 2015; 6(14):12020-34.
36. Kafil V, Omid Y. Cytotoxic impacts of linear and branched polyethylenimine nanostructures in A431 cells. *BioImpacts* 2011; 1(1):23–30.
37. Brunot C, Ponsonnet L, Lagneau C, Farge P, Picart C, Grosogeat B. Cytotoxicity of polyethyleneimine (PEI), precursor base layer of polyelectrolyte multilayer films. *Biomaterials* 2007; 4:632-40.
38. Xiao Y, Shi K, Qu Y, Chu B, Qian Z. Engineering Nanoparticles for Targeted Delivery of Nucleic Acid Therapeutics in Tumor. *Molec Ther Meth and Clin Development* 2019; 12:1-18.